ICAS Paper No. 70-14

SOME PROBLEMS AND FEATURES OF TRANSONIC AERODYNAMICS

by
H. H. Pearcey, Deputy Chief Scientific Officer
and
J. Osborne, Sr. Experimental Officer
National Physical Laboratory
Teddington, U.K.

The Seventh Congress of the International Council of the Aeronautical Sciences

CONSIGLIO NAZIONALE DELLE RICERCHE, ROMA, ITALY / SEPTEMBER 14-18, 1970

Price: 400 Lire

SOME PROBLEMS AND FEATURES OF TRANSONIC AERODYNAMICS

H.H. Pearcey and J. Osborne
National Physical Laboratory, Teddington U.K.

Abstract

The repercussions of mixed, transonic flows are now known to be legion. For example, the shock waves that such flows often generate, and the associated drag and boundary-layer separations, have some part:-

in limiting not only the cruise performance of a wide variety of swept-wing aircraft but also their usable lift throughout their speed range, and hence their stalling speeds, manoeuvrability, etc;

in limiting not only the forward speed of helicopters and other rotorcraft but also their lifting capability, and hence their manoeuvrability, performance in hover, payload and range;

in the flow not only through fans, compressors and turbines, but also on the lips of subsonic engine nacelles from static conditions on the runway to steady flight at cruise speed.

Many problems of practical importance thus arise for which the aerodynamics are still not predictable mathematically. However, phenomenological studies of the flow processes involved have consistently led to evolutionary progress in design as is shown by typical examples. Attention is also drawn to some of the flows that are still not at all well understood in spite of their practical importance.

1. Introduction

For the purpose of this paper we are using the word "transonic" to describe the aerodynamics that are associated with the co-existence of subsonic and supersonic flows on the wings, nacelles, rotor blades or other components of aircraft and their engines.

We shall be concerned with the case in which the supersonic flow is local and embedded within a main subsonic flow (Fig.1(a)), rather than that for which the supersonic flow surrounds an embedded subsonic region (Fig.1(b)), although some features of the one carry across in some degree to the other. The sketches represent two-dimensional aerofoils but can also be used conceptually for axi-symmetric bodies and annular aerofoils. Furthermore, the broad concepts apply to many cases in which the velocity of the "main flow" has been obtained by resolution. (Fig.1(c) and (d)). Thus, for a swept-back wing, considered for the moment as an ideal yawed wing, the main flow in the sense that we are using it is characterised by the component, M_N, of the stream speed (or forward speed) normal to the wing isobars. Again, we shall take the case in which the supersonic flow in the resolved (and effective) sense is embedded in the main subsonic flow (in the resolved sense) (c), rather than that in which the effective supersonic flow surrounds the effective subsonic flow (d).

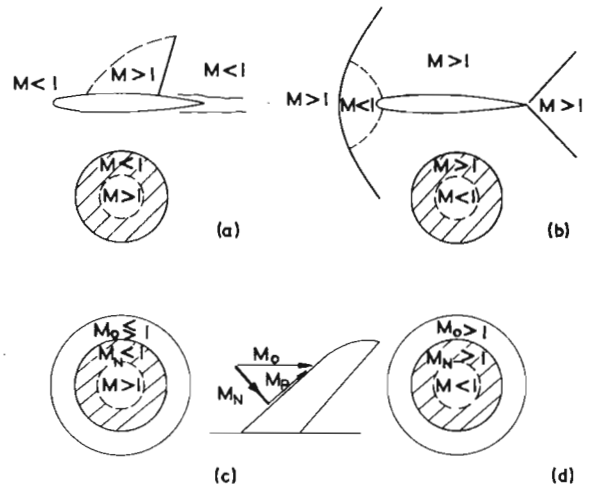

Figure 1. Types of transonic flow; the inner circles represent the embedded regions, hatched areas the effective surrounding flow.

It is of course largely because we have continued to be concerned with features of transonic flows on swept wings as they have been developing as a class that transonic aerodynamics as a discipline has been kept alive and has so strongly revived in recent years. Many of the flow phenomena that we now encounter are special to the three dimensional environment, and owe much of their complexity to this, but there are also many that were first encountered and revealed in the study of aerofoils at high subsonic speeds. Indeed, aerofoil research continues to give an effective lead into many of the problems with which we have to contend in order progressively to improve the performance of this class of aircraft; in many cases it is the most realistic starting point, but it must always be remembered that it may only be a starting point to something more complex and practical, as recently re-iterated by Küchemann.(1)

Of very considerable interest, also, is the fact that some of the most recent studies of transonic aerodynamics have opened up in the context of helicopters and rotorcraft, where the "main flow" is compounded from the forward and rotational speeds (Fig.2) - just as it was in the case of the propeller that gave birth to the subject as we have come to know it at the hands of Dryden, Stack and their colleagues at NACA and C.N.H. Lock our mentor at NPL. Just as Lock, Hufton, Pankhurst and their colleagues were able to start from the transonic characteristics of two-dimensional aerofoils to synthesise a strip theory for propellors(2) so current helicopter researchers are finding the same starting point indispensible in tackling the much more complex aerodynamics of the helicopter rotor; one can sense already a similar fruitful interaction developing between the work on the idealised aerofoil and the complex design.(3,4)

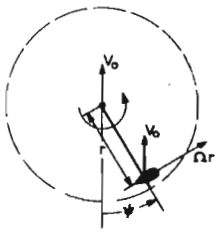

Figure 2. Velocity components in plane of helicopter rotor.

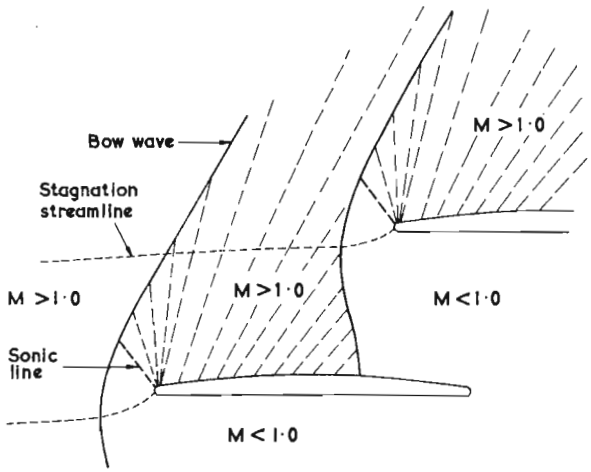

Figure 3. Flow past transonic compressor blades.

The engine designer has been concerned - with much greater continuity he would justly claim - with similar problems on his compressors, turbines and fans[5,6] (Fig.3). The dominance of the rotational and radial components have been such that the direct approach to the actual rotor has usually been necessary, but it is of interest to note the revived interest in oascade research in recent years - the counterpart to aerofoil research in the other contexts - and we look forward to a growing interchange of ideas here too. The engine and airframe designers have also, of course, been continuously, and in concert, dealing with problems of transonic flows in the various and repeated processes of acceleration and deceleration that they have to achieve into and through the engine intake and through and out of the nozzle[7,8,9], and in the varying degrees of acceleration and deceleration that they have to accommodate around the nacelle lip and afterbody in adjusting to the various conditions of intake mass flow and jet thrust (Fig.4).[9]

Indeed, one of the earliest observations of the fact that significant regions of embedded supersonic flow can occur without any identifiable repercussions of shock-waves has been recorded in this context by Küchemann and Weber[10]. So, the phenomena that we now tend to describe as "peaky flows" have their origins as much in the nacelle field as in the aerofoil field. "Interference" between the airframe and the engine, its pods, pylons and jets, is also a frequent source of acceleration to local supersonic flow.[11,12,13]

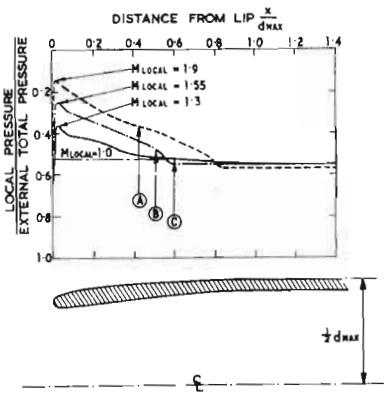

Figure 4. Shock-free transonic flow on an intake cowl, M_o=0.9; curves A,B,C represent increasing mass-flow ratio (Ref.9)

Transonic flows - in one guise or another - are thus of considerable importance in practical and current problems of aircraft design; they will remain so for as long as can be foreseen for the very simple and self-evident reason that, quite apart from the accelerations generated by the presence of a body of finite volume, all the processes of producing lift and thrust depend on accelerating and decelerating the flow to create the suctions and pressures required on the appropriate surfaces. These processes will be constrained whenever the acceleration develops local supersonic velocities from which the necessary deceleration cannot be achieved without shock waves. It is very well-known that many of the operational limits to speed, range, payload, manoeuvrability and so on arise in just this way.

We want, as the main theme of this paper, to remind you of some of these limitations and to do this by illustrating some of the forms in which the transonic flow phenomena are involved. We shall try also to keep running through the dissertation two subsidiary themes. The first of these is that the designer, in the evolutionary stages of removing the limitations imposed by transonic flows, has had to lean even more heavily than usual on phenomenological studies of the flow processes and their implications and less on quantitative parametric evaluation of their influences, because these processes involve a mixture of elliptic and hyperbolic regions (as far as the differential equations of motion are concerned), singularities and non-linearities and large perterbations; they are not isentropic, irrotational or inviscid, and, indeed, are often separated and/or unsteady. We are delighted that a powerful new mathematical attack is now being mounted across the world[14,15,16,17], is already bearing fruit and is greatly helping in the process of understanding and also of design (Fig.5(b)). We feel confident that this will ultimately remove much of the empiricism at present involved in design, especially if those of us concerned with the practical phenomena can develop a lively conversation with the mathematicians.

In order to illustrate what we mean by evolutionary progress through phenomenological studies, purely by way of example and as we feel might be expected of us, we shall make some reference to what can be done to control the development of the local supersonic flow to produce the so called peaky flows (Fig.5(a)).

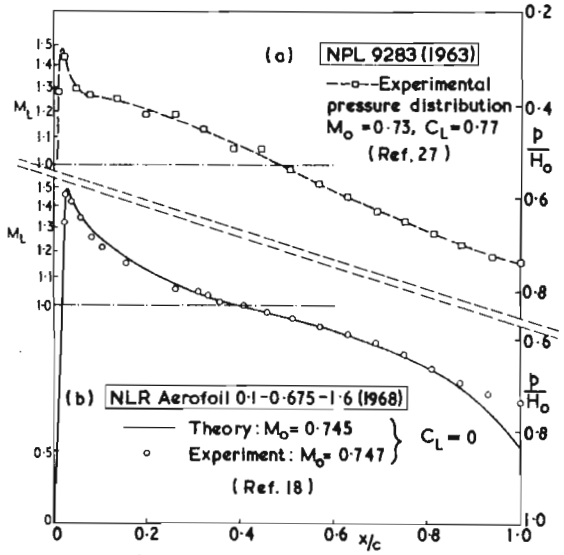

Figure 5. Shock-free flows on aerofoils designed: (a) empirically, (b) theoretically.

As the second subsidiary theme to the dissertation we shall draw attention from time to time to the practical importance of some of the flow processes that are still not at all well understood, even phenomenologically. In this context we shall concentrate, by way of example again, on the extremely small embedded regions of supersonic flow that tend to occur at fairly low free-stream speeds when the acceleration - usually at the leading edge - is very rapid. These small regions can certainly exert a strong adverse influence, and this is often through an interaction between the shock wave and the boundary layer (Fig.6). At some point, however, the distinction between this type of shock-induced separation and the classical low-speed type of separation becomes blurred, and it is the nature of the transition from one to the other that has not been much studied in spite of its many repercussions.

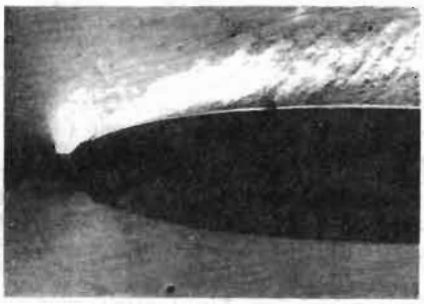

Figure 6. Very small region of local supersonic flow with significant repercussions; M_N=0.45, incidence=11.5°.

2. Transonic Flows on Swept Wings

The paper that Mr. A.B. Haines[13] presented to the last ICAS Congress in München two years ago provided an excellent example of how progress in the design and development of this class of wing for transport aircraft has depended on a full understanding of the flow processes involved. Similar accounts have been given for the specific case of the Harrier combat aircraft by Mr. J. Fozzard - who is speaking at this Congress - Mr. C. Bore and their colleagues of Hawker Siddeley's.[9] With these accounts available of the all-important practical processes of working from basic concepts to real designs and, in particular, from concepts derived from aerofoil research to the actual three-dimensional wing, we feel free - in this very broad discussion of how transonic flows react on aircraft design and performance - to return to some of these basic concepts and to do this by reference to the idealised case of the two-dimensional aerofoil.

Thus, in the central diagram of Fig.7, we use an (M,C_L) plane in which the Mach number is taken as the component, M_N, normal to the leading edge of the wing and the lift coefficient as the load on local sections of the wing normalised by this same component (i.e. $C_{L_N}=L/\frac{1}{2}\gamma p M_N^2 c$). The loci L_1, L_2 (corresponding to two constant values of M^2C_L) represent the combinations of aircraft speed and section loading required to sustain steady flight at two altitudes, namely, sea level and a typical value for cruise (40,000 ft.)

In juxtaposition with these loci are boundaries beyond which certain transonic flow phenomena would be encountered on the two-dimensional aerofoils representing the sections normal to the isobars of the wing; the flow boundaries reproduced here are those beyond which (1) the flow becomes supercritical and hence transonic according to our definition i.e. the main subsonic flow encloses an embedded region of local supersonic flow, (2) the drag rises rapidly due to the onset of wave drag and (3) the repercussions of shock-induced separation begin to be felt. The object of this juxtaposition is to provide examples of operational limits that are related to the adverse flow phenomena. We shall proceed to mention some of the limitations and to discuss some of the flow phenomena involved.

At A, the minimum speed for take off and landing is related to the low speed stall, and in many cases transonic flows are already involved, but, as mentioned earlier, to a degree and in a form that are not yet at all well understood.

At B, the maximum speed that can be maintained at sea level, there is no doubt about the involvement of shock-wave drag and shock-induced separation; their development with increasing Mach number has been extensively studied and needs no further comment here. However, mention above of the Harrier is a reminder that some of the important recent trends in aircraft design for low level flight have pressed us harder and harder in our studies of transonic flows at the higher lift coefficients appropriate to flight at altitude[9]. For example, the requirement for sustained low level flight at high speeds, the development of STOL and VTOL capabilities, and the introduction of variable sweep can all lead the designer towards higher wing loadings. The locus L_2 is then relatively high up the (M,C_L) plane and its intersections with the flow boundaries more restrictive on performance at cruise altitude, or, conversely, more demanding with respect to design. The NPL 3111 section[19,20] for which the flow boundaries are shown in Fig.7 was developed for a military transport specification in 1964 that was to have

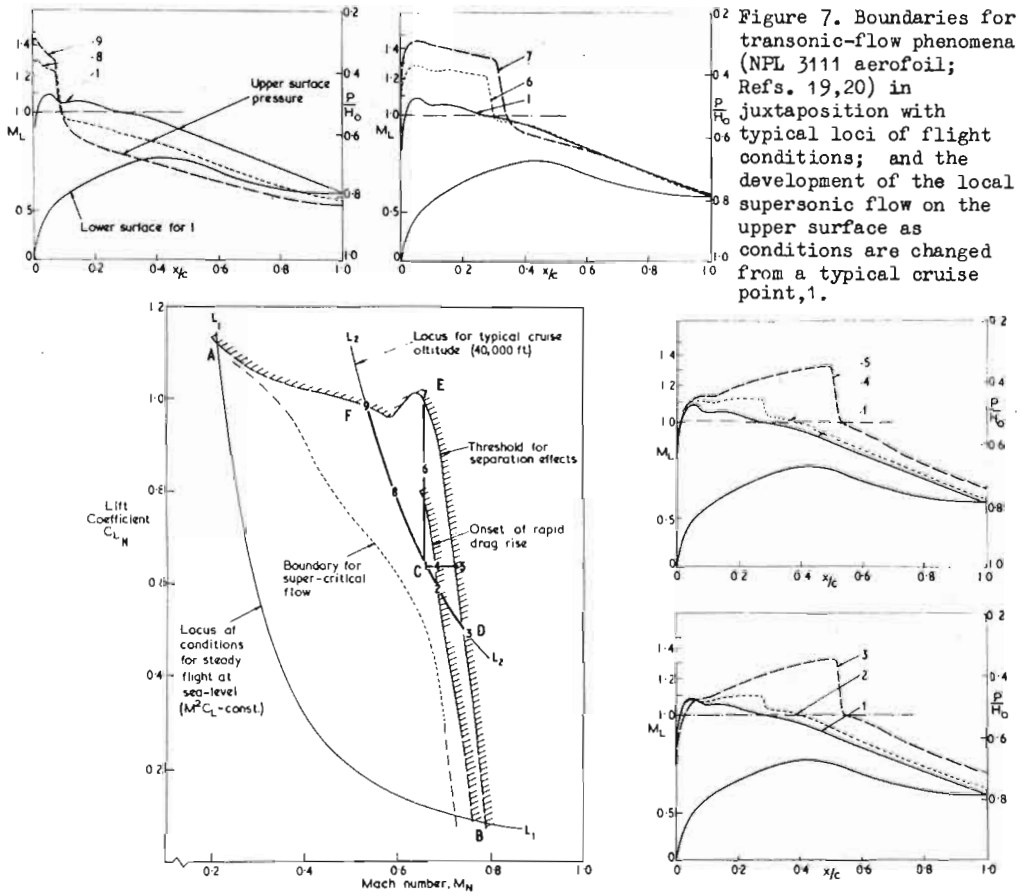

Figure 7. Boundaries for transonic-flow phenomena (NPL 3111 aerofoil; Refs. 19,20) in juxtaposition with typical loci of flight conditions; and the development of the local supersonic flow on the upper surface as conditions are changed from a typical cruise point,1.

had deflected thrust engines for STOL; it provides, therefore, a useful example of the pressures that have been mounting in this respect and we shall be looking at the types of flow that it generates in a little more detail.

But, first, we should continue our enumeration of the operational limits that are related to transonic flow phenomena. At C, the cruise speeds that give the best range, payload and block-speed are related to the onset of wave drag. At D, the maximum buffet free speed at cruise altitude is related to the onset of shock-induced separation. At E, the maximum loading that can safely be used at cruise speed for manoeuvre or that can be tolerated in gust encounter is also related to the onset of shock-induced separation. Finally, at F, the minimum buffet free speed at cruise altitude is related to a type of separation that may be shock induced and is certainly strongly influenced by the presence of local supersonic flow.

In practice, the limiting flight envelope for manoeuvres, gusts, etc., at cruise altitude will lie somewhere beyond the curve DEF; this curve represents the first onset of the effects of shock induced separation (e.g. the divergence of trailing edge pressure) and therefore a threshold beyond which serious repercussions build up progressively, with the degree of permissible penetration depending on the rate at which the adverse flows develop and on aircraft response, design limits and so on. The limiting envelope will, however, bear a close relationship to this threshold and, in particular, will reflect the progressive rapid decrease and ultimate disappearance of available loading as speed is increased and decreased from C.

For the NPL 3111 section, the point 1, (Fig.7) was chosen as a suitable cruise point. The required relatively high value of C_L was obtained by combining some rear loading with a supercritical, shock free upper-surface flow. However, considered from the point of view of cruise alone, the design was conservative in at least three respects, namely, (1) it lies significantly to the left of and well clear of the shock wave drag rise boundary, (2) the region of high velocity on the upper surface does not extend very far aft and (3) it involves only a mild form of peaky flow. This conservatism was necessary in order to meet stringent requirements for buffet-free C_L at E and manoeuvrability at lower speeds; it illustrates a general point of growing importance. As the trends mentioned above produce growing demands for high lift coefficients at cruise, and as the possibilities of meeting these are provided by advances in section and wing design, so the problem of providing adequate margins of usable lift coefficient over the Mach number range DEF becomes more and more difficult.

The incremental lift coefficients required for manoeuvre, like CE, increase in proportion to the value of the cruise C_L; for each advance ΔC_L in cruise C_L an increase $n\Delta C_L$ is required in usable C_L, with n being significantly greater than unity and depending on the role of the aircraft in question. Thus the achievement of controlled development of the local supersonic flow over the

whole of that part of the (M,C_L) plane enclosed by the locus L_2 and the boundary DEF, say, assumes rather more importance in the overall design process than does the design for some particular cruise point. Correspondingly, in research, we have to place greater emphasis on optimising supersonic flow developments for a range of conditions than on achieving particularly favourable flows at one condition, and to be more concerned with understanding, delaying and alleviating the effects of shock induced separation than with delaying shock wave drag.

3. Accelerations and decelerations in the local supersonic flow; the peaky concept

The distributions of surface pressure (and local Mach number) reproduced in the peripheral diagrams of Fig.7 illustrate how the local supersonic flow develops for the NPL 3111 section as conditions change from the cruise point C, or 1, within the region contained by the locus L_2 and the boundary DEF. They show, in particular, that the shock-free deceleration is obtained only at conditions near C itself. Shock waves develop and become limiting in the sense that they produce boundary layer separations of unacceptable severity as the boundary DEF is crossed to points like 3, 5, 7, 9.

Two broad features of these limiting distributions are of special interest in the present context: (1) the shape changes as one moves around the boundary DEF, from one (point 3) in which the local supersonic flow is accelerating right back to the shock (albeit mildly in comparison with some older aerofoil designs) to one in which some deceleration is achieved (points 7 and 9). (2) the limits occur for shock waves of approximately the same strength and upstream local Mach number irrespective of chordwise position and of the sign and strength of the upstream pressure gradient; in other words the limiting phenomenon is coupled to the magnitude of the deceleration through the shock itself rather than to the overall deceleration from leading edge to trailing edge.

To consider in more detail this coupling to the shock-wave pressure rise it would of course be necessary to take into account certain parameters that are known to influence the value of the pressure rise - and that of the upstream Mach number - that is critical for separation.[21] For a real wing, the sweep of the shock front itself, and still other factors, have also to be taken into account. Nevertheless, and again in broad terms, the greater the degree of deceleration that can be achieved isentropically upstream of the shock, then the greater tends to be the lift that can be achieved at the limiting condition. This is illustrated in the sketch in Fig. 8 which indicates the degree to which the loading was greater at E (point 7) for the NPL 3111 section than it would have been if the flow had been accelerating back to the shock (as it does on some aerofoils) and less than it might have been if a stronger peaky flow still could have been invoked - by a change in leading edge design or surface slope distribution, say. Any such change would of course also effect the development of the local supersonic flow at other points around the limiting boundary, and maybe near point C also; in some cases the change

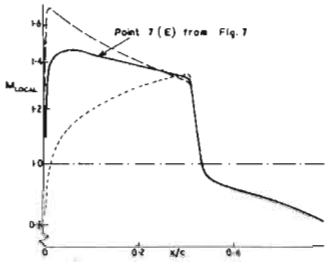

Figure 8. Decelerating supersonic flow provides extra lift at limiting shock conditions.

would be favourable and in others probably unfavourable (and this applies particularly to points near F). This illustrates the nature of the compromise that the designer has to strike, and indicates that the decelerating, or peaky, flow cannot be exploited to the same degree at all points. Rather, it has to be invoked in such a way as most favourably to influence the overall compromise between various points on the limiting boundary and between this overall boundary itself and the cruise conditions.

To look back a decade, it was precisely this idea that we had in mind in originally drawing attention to these favourable peaky flows[21,22] and to some of the aerofoil design features that lead to their development. Observations of peaky flows under apparently random conditions had been reported from time to time for many years before that[10]; what we did was merely to attempt some sort of classification and to suggest what might be done to exploit the favourable flows in design. We also tried - and this was probably at least of equal importance at that time - to warn about what should be done to avoid the contrasting, unfavourable, so called, triangular flows.

Several other people have had similar ideas since then and have made more significant contributions to the subject. Many of the subsequent developments are well known, but it will suit our main theme to illustrate some of them. It was of great encouragement to us to get confirmation at a relatively early stage that our classification of the manner in which the contrasting types of flow relate to the crest criterion for drag rise (Fig.9, left) was borne out on certain actual aircraft[23,24,25]. The high peaks, or triangular types of flow, that were causing the pronounced supercritical drag creep on local sections of an early version of one of these (Fig.9, right) were first identified by section tests and then converted to mildly peaky flows through two successive leading-edge modifications. The insert diagrams show how the shock strength was reduced progressively by these changes. The relative changes in drag on the respective two-dimensional aerofoils were well reproduced in flight when the leading-edge of the appropriate part of the span was modified during the flight development programme. Fig.10 is an illustration (from model tests) of an isentropically decelerating supersonic flow spreading out over the full chord - as speed is increased through the cruise value - at one spanwise station of another of the swept wings in question. Mr. Haines' paper[13] includes another example of how flows similar to that shown at E of Fig.7 were achieved on an actual swept wing. The particular section shape that was used as a basis for that swept wing was the NPL 3112, one of those represented in Fig.11. The object of Fig.11 is to demonstrate how the drag rise conditions achieved

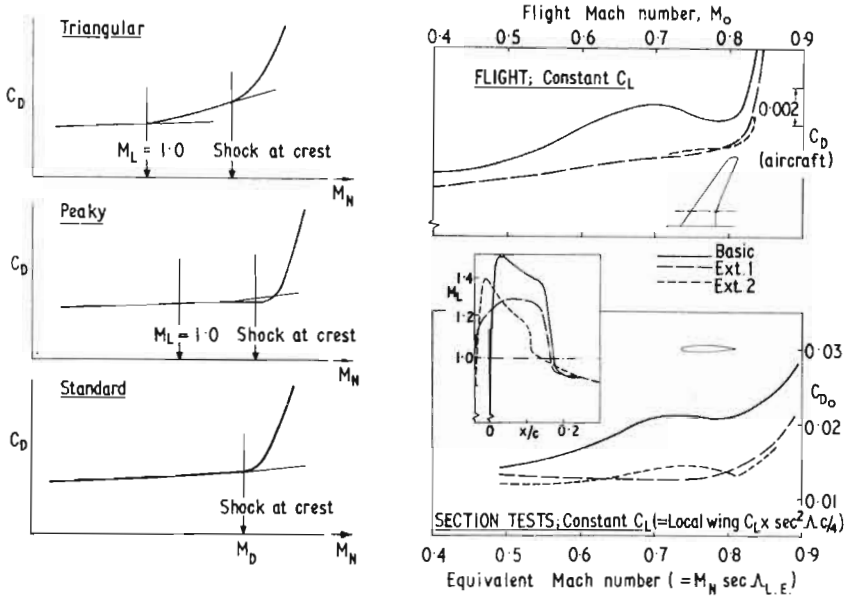

Figure 9. Classification of drag curves (left) and (right) its relevance illustrated by a comparison between section tests and flight (Ref. 25).

on sections tested as part of the development processes of certain swept wing designs in the past decade have compared with a "standard" datum series of aerofoils represented by the chart[26]. The progress achieved has not by any means all been associated with peaky flows, but it has been evolutionary and based on a phenomenological studies of the flow processes that were invoked.

We were also encouraged, by our own results of achieving partial isentropic recompressions from relatively high local Mach numbers, to pursue the possibility of obtaining complete recompressions that were effectively shock free on aerofoils of practical shape, and to demonstrate the nature of the gains that these might offer. These goals were achieved by an interative empirical process that produced the NPL 9283 aerofoil; some of the results[20,27] are included here in Fig.5(a) (pressure distribution) and Fig.11 (drag rise M_D, C_{L_D}).* The arrow drawn along a line of constant $M^2 C_L$ illustrates the magnitude of the gain that this section could offer over its "standard" counterparts in sustaining the same wing loading in steady flight at the same altitude. On the assumption that the corresponding flows could be achieved with similar isobar patterns on corresponding swept wings, the comparison also remains valid after transposition to their respective swept wings; the yawed wing transformation implies:

$$M_N = M_o \cos\Lambda, \quad C_{L_N} = C_L \sec^2\Lambda; \quad \text{i.e. } M_N^2 C_{L_N} = M_o^2 C_L$$

For a given sweepback Λ, the magnitude of the gain in M_N offered by the NPL 9283 aerofoil over its standard counterpart would be factored by $\sec\Lambda$ (and this of course applies to the other aerofoils represented in Fig.11).

The most important impetus to the concept of shock-free supercritical flows came from Nieuwland and his colleagues at NLR in Holland[14,18,28], who finally proved that such aerofoils were mathematically as well as physically realistic,

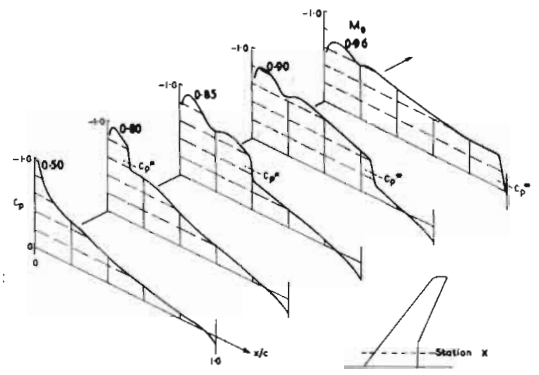

Figure 10. Decelerating supersonic flow upstream of the shock at station x of a swept wing.

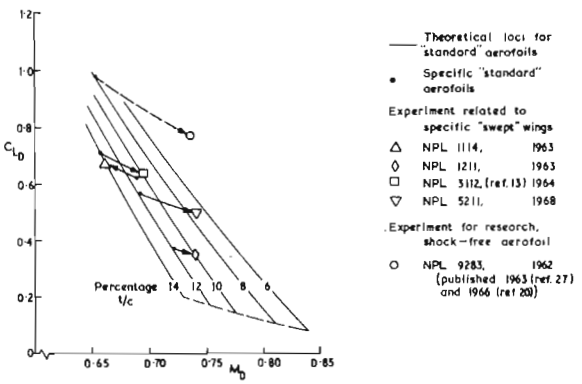

Figure 11. Drag rise conditions (M_D, C_{L_D}) observed on actual aerofoils (symbols) compared with theoretical values (dots) for corresponding "standard aerofoils" (roof-top back to 0.4 chord); the direction and length of the arrows (on lines of constant $M^2 C_L$) reflect relative merits.

* The drag of this section at its drag rise conditions was no greater, in fact slightly less, than that of a corresponding roof-top aerofoil at its lower drag rise Mach number[27].

numerically derivable, and experimentally verifiable. One of their early results[28] for a symmetrical aerofoil at zero lift is reproduced in Fig.5(b); there is a striking similarity between this particular solution and the flow that we had obtained by an empirical design process on the upper surface of the NPL 9283 aerofoil (at C_L approaching 0.8). Nieuwland's work provides a much broader range of solutions, of course, and at this Congress his colleagues from the NLR are demonstrating further progress by presenting solutions for the lifting case.

The complete shock-free flow can be seen merely to be a special case of the perfectly general embedded supersonic region on a convex surface it one considers the internal structure of this region on the basis of its characteristics and the wave-like, infinitesimally small disturbances carried on them (Fig.12(a)). It can be proved[29]

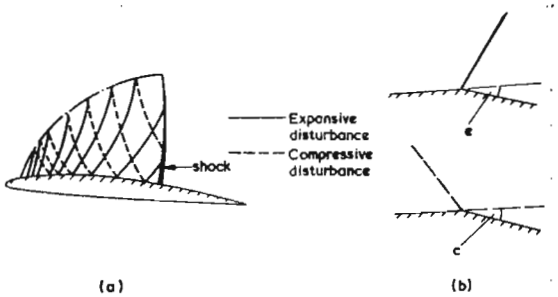

Figure 12. Disturbances on characteristics and their contributions to convex flow deflection.

that the disturbances on the outgoing family are expansive and those on the incoming compressive.

It should be noted (Fig.12(b)) that both types of disturbance provide a convex turning at the surface, i.e. e(x) or c(x). The angular deflection between the upstream sonic point, x_s, and a given downstream point, x_1 on the surface is then:

$$\phi(x_1) = \sum_{x_s}^{x_1} e(x) + \sum_{x_s}^{x_1} c(x)$$

$$= E(x_1) + C(x_1), \qquad (1)$$

where, $E(x) = \sum_{x_s}^{x} e(x)$, $C(x) = \sum_{x_s}^{x} c(x)$

It can also be shown that the Prandtl-Meyer angle of the flow at the given point on the surface is:

$$\omega(x_1) = E(x_1) - C(x_1) \qquad (2)$$

Equations (1) and (2) are illustrated graphically in Fig.13(a) and (b), respectively.

The distribution of local Mach number, M(x), is uniquely related to $\omega(x)$ which emerges as the difference between the integrated strengths of the expansive and compressive disturbances, each of which is often large compared with the magnitude of $\omega(x)$ itself. Whether the flow is accelerating or decelerating locally then depends on the relative magnitudes of the wave strengths $\partial E/\partial x$, $\partial C/\partial x$ locally.

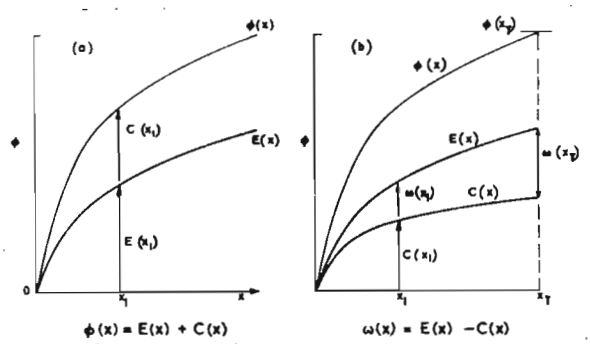

Figure 13. (a) the summation (flow deflection) and (b) partial cancellation (residual acceleration) of disturbance waves.

The magnitude of $\omega(x_T)$ at the end of the sonic region, x_T, depends on the relative integrated strengths, i.e.

$$\omega(x_T) = E(x_T) - C(x_T)$$

The shock free case,

$$\omega(x_T) = 0,$$

corresponds, from equations (1) and (2), to

$$E(x_T) = C(x_T) = \tfrac{1}{2}\phi(x_T) \qquad (3)$$

i.e. the integrated strengths of the two families of waves just cancel, with each having contributed equally to the convex turning. This is illustrated, using one of Nieuwland's theoretical results, in Fig.14.

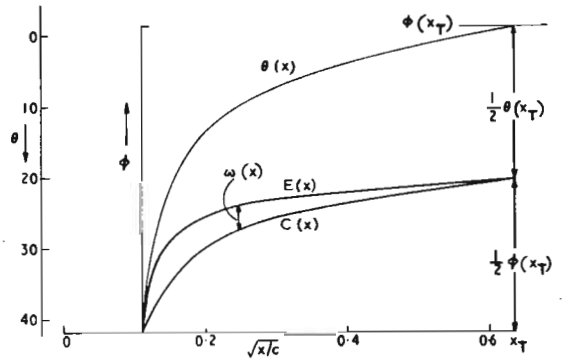

Figure 14. Complete wave cancellation for shock-free flow (from Nieuwland's results).

Equation (3) gives one necessary condition for the flow to be shock free, bearing in mind also that sonic points, x_S, and, x_T, must be compatible with the upstream and downstream subsonic flows respectively. Two other necessary conditions can be postulated, namely, (1) that due to Spee[18] which ensures that extraneous disturbances, and in particular those originating downstream of the supersonic region, must be able to turn and to propagate through the region with finite velocity relative to the aerofoil (i.e. without coalescing into a shock), and (2) that which ensures that the characteristics of the incoming (compressive) family do not coalesce to form an internal shock. (This condition is satisfied at the surface if $\partial E/\partial x$ is positive, i.e. if the strength of the compressive disturbance is never quite as strong as

a simple-wave compression). We suggest that these three necessary conditions can be considered as representing respectively: continuity of flow direction and other flow properties with the upstream and downstream subsonic flow; the absence of shock formation due to "piling up" of disturbances originating outside the local supersonic region; and the absence of internal shocks caused by the coalescence of the inherent compressive disturbances. We are not aware of any demonstration that, as a set, these conditions are not also sufficient. (There could, however, be some interdependence between them).

Seen in this light, the wave cancellation process for the shock-free flow is no different in principle from that which is always present, but is particular in the sense that it is complete and leaves no residual $\omega(w_1)$ at the end of the supersonic region, and in the sense that a potential-flow solution should therefore be possible. When conditions of upstream Mach number, surface slope, etc., change progressively from those which gives the shock-free flow, one might expect the residual $\omega(x_T)$ to increase slowly and progressively from zero, and the shock-free flow therefore to have a continuity of neighbouring flows with terminating shocks growing progressively in strength. This is in line with the experience that has so far not exposed any of the inherent instabilities that had at one time been predicted or any of the critical influences often ascribed to the presence of a boundary layer.

The above explanation of the interaction between the two families of waves is not inconsistent with earlier ones, but, we believe, avoids the element of artificiality involved in considering the compressive disturbance as the difference between the actual expansion and the hypothetical simple-wave expansion from the convex surface that would occur for uniform upstream flow[30] or in considering the addition of an arbitrary expansive wave to an existing flow and then its repeated reflection at the sonic line and surface[21].

By adding a curve of $\frac{1}{2}\phi(x)$, one can convert Fig.13(b) into Fig.15 that is equivalent to that used[21] to illustrate the principle of connected points, but with all the ordinates halved; an

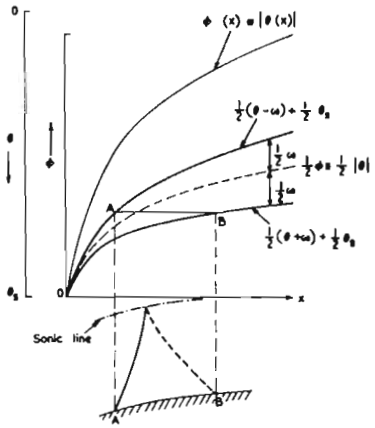

Figure 15. Connected points.

ordinate of surface slope, θ, is also included. Horizontal lines connecting points A and B in Fig.15 (upper) have

which is the condition that A and B on the surface are connected in the sense that the compressive disturbance reaching B is the reflection from the sonic line of the expansive disturbance that leaves A. The arguments about the relative dispositions of surface curvature, and of the rapid expansions (i.e. high values of $\partial E/\partial x$) that are required to achieve the desired downstream decelerations ($\partial C/\partial x > \partial E/\partial x$) then follow in the same way as before[21,30].

It is of interest now to return briefly to the nature of the problem involved in controlling the development of local supersonic flow for the wide range of conditions of Mach number and lift coefficient encountered on a typical swept wing aircraft; this is done in Fig.16 by reference to the limiting conditions 3, 5, 7, 9 on the boundary DEF for the NPL 3111 aerofoil (Fig.7).

The left-hand scale of Fig.16 gives the surface slope, with 90° corresponding to the leading edge. A portion of the surface slope distribution, $\theta(x)$, of the aerofoil is reproduced in each of the other diagrams corresponding to that part between the forward sonic point x_s and the terminating shock x_T for each experimental result. The degree of convex

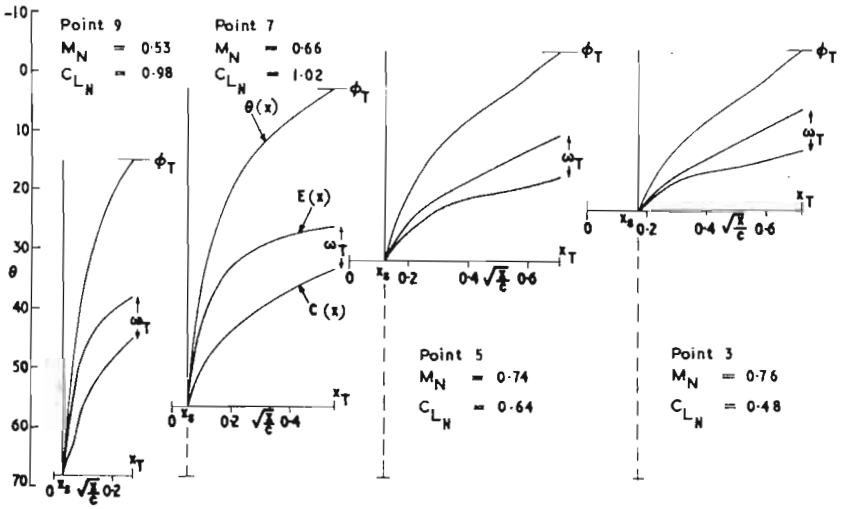

Figure 16. Wave-cancellation analysis applied to the limiting conditions (3,5,7,9) of Fig.7.

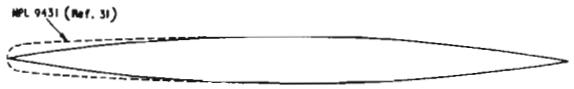

Figure 17. Round-nosed aerofoil designed for shock-free, peaky flow at M_N=1.0, C_L=0.

turning increases from 27° for case 3, to 54° for case 7 and 53° for case 9 as the forward sonic point moves on to the highly curved leading edge with increasing C_L and decreasing M_N. The curves of E(x) and C(x) indicate the proportion of this turning that occurs respectively on the expansive and compressive families of waves. The most striking feature is perhaps that the residual $\omega(x_T)$, and hence the final shock strength, is held respectively to 6.8°, 7.1° and 6.4° by virtue of the more complete wave cancellation for cases 7 and 9. The more rapid expansion on the forward part of the chord and the subsequent, reflected, compression is an essential part of this; it can be seen in greater contrast by its absense for cases 3 and 5. Nevertheless, for these latter cases the near complete cancellation that was achieved for the early part of the supersonic region contributed to the rather mild accelerations in these cases (compared with older types of aerofoil).

Another feature that can be inferred from these diagrams is that the wave cancellation and compression that has to follow the initial rapid expansion in order to keep $\omega(x_T)$ small requires a certain chordwise distance; thus too rapid an expansion at low stream Mach numbers, before the supersonic flow has spread rearwards, could lead to stronger shocks than might otherwise occur.

It is obvious from analysis of this kind that, in addition to careful design of the surface slope distribution, the necessary compromise over the wide range of conditions requires also a careful control of the leading-edge shape and of the position of the sonic point on it; this illustrates one of the gaps in achieving this compromise at this stage, namely, an incomplete knowledge of how the variation of stagnation point and sonic point depend on such variables as Mach number, incidence and leading-edge shape[30].

After this description, which presents the distribution of $\omega(x)$ as the difference between two larger quantities carefully contrived to keep the residual $\omega(x_T)$ as small as possible, it is salutary to recall that the lift attainable is related to the integral of $\omega(x)$ along the surface.

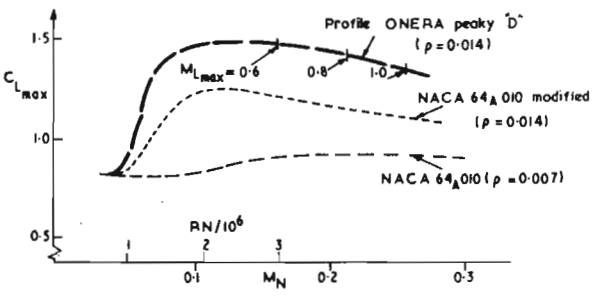

Figure 18. Low-speed $C_{L_{max}}$ for a peaky aerofoil and others (Ref. 33) (ρ=leading-edge radius and chord).

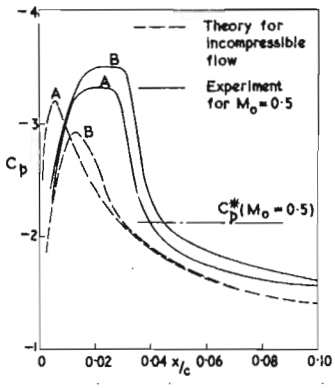

Figure 19. Effect of Mach number on the relative merits of two aerofoils at high C_L.

The evolutionary progress that has followed from understanding how best to exploit the controlled development of local supersonic flows at high subsonic speeds (e.g. FED of Fig.7) has been compatible with progress in certain other areas and, indeed, has stimulated some of this progress. For example, Graham[31] designed an aerofoil with large leading-edge radius (Fig.17) to have a "shock-free", peaky flow at M_N=1.0 and a pressure drag (i.e. wave drag) some 8% lower than that of the inscribed biconvex aerofoil. More generally, Wilby[32] has shown that the round leading-edges that produce good peaky flows at high subsonic speeds do not produce any higher drags at moderate supersonic speeds than do sharp leading-edges. At the other extreme of the speed range, Erlich[33] has recently shown that an ONERA peaky aerofoil[34] has significantly better $C_{L_{max}}$ characteristics (Fig.18) than a conventional profile of the same thickness/chord ratio and leading-edge radius. However, this does not necessarily mean that for any given peaky aerofoil $C_{L_{max}}$ remains uniformly high over the whole range of speeds up to the point E, say, on Fig.7. For example, of the two aerofoils represented by Fig.19, A would exhibit the higher $C_{L_{max}}$ at low speeds because of the lower peak suctions for such conditions (indicated by incompressible theory). But, the relative merits of the two aerofoils are reversed as M_N is increased to 0.5 and the local supersonic flow develops on the nose to produce a stronger shock for B than for A.

Note that these significant changes occur in the first 4% of the chord and so we turn naturally to our second subsidiary theme.

4. Very small, leading-edge regions of embedded supersonic flows

The surface pressure distributions presented in Fig.20 have been selected from a set taken at very close intervals of M_N for an aerofoil fixed at 12° incidence. They demonstrate how the development of these miniscule regions (the scale in relation to the leading-edge profile is illustrated by Fig.6) often reproduces to a quite remarkable degree many of those features that have been so extensively studied for the much larger regions that occur at lower values of incidence and higher values of stream Mach number with chordwise extent and height that are both of the same order of magnitude as the aerofoil chord itself.

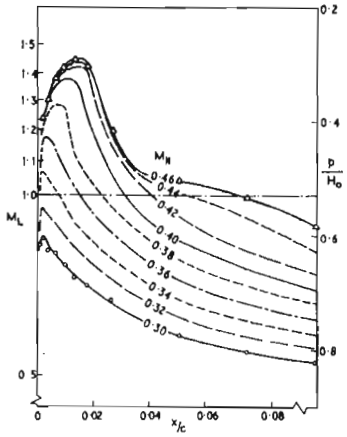

Figure 20. The development of a very small region of embedded supersonic flow on the leading-edge of an aerofoil at 12° incidence (upper surface pressures).

The change in shape from the subsonic distribution occurs progressively as the local supersonic flow accelerates further and further around the leading-edge. A shock develops and seems to generate - in the range M_N=0.42 to 0.46 - the type of separation for which the bubble expands rapidly as the supersonic tongue first extends along it[39]. Unlike their larger counterparts, little is yet known about the details of these flows except that they exert a strong influence of practical significance in many types of application. The manner in which they depend on leading-edge shape and bridge the transition from the classical low-speed stalling situation to the fully developed shock-induced one should be an especially rewarding subject for research. It could have a strong bearing on scale effects[39], for example, on hysteresis[33] and on the effects of rate of change of incidence[3]. There could be extremely important effects of sweepback also (see below). Unfortunately, experimental techniques such as optical flow visualisation become more difficult on the scale of model that we normally test, and such questions also arise as to what is the appropriate simulation of transition position to represent full-scale conditions. An extension of the inspired technique used by Erlich[33] to reproduce leading-edge flows at an enlarged scale would seem to be needed.

In the meantime, the results shown in Fig.21 can throw some light on the nature of the transition from low-speed to shock-induced stall for one instance. They were obtained on the same aerofoil as the results in Fig.20, in the same transonic wind tunnel (36 in. x 14 in; 0.9m. x 0.35m.) and with the same chord length (10 in; 0.25m.) The Reynolds numbers were therefore very low for the lowest Mach number, 0.1. In separating out the effects of increasing Reynolds number and Mach number (which were increasing simultaneously in the experiments) reference to Fig.18 and also to earlier work[35] is of considerable help because the initial increase in $C_{L_{max}}$ (under the influence of Reynolds number) is there more pronounced and shows the subsequent dominance of the Mach number effects in greater contrast. The initial increase, with increasing peak suction, is just detectable in Fig.21 for points 1, 2, 3, but the overiding effect of Mach number then becomes evident, with the peak suction already falling at point 4, just before the flow becomes supercritical. This turning point occurs for similar values of local Mach number (again, before they reach 1.0) to those observed in the other tests. The downward trend continues through points 5 and 6; the peak suction is falling in terms of pressure coefficient, C_p,

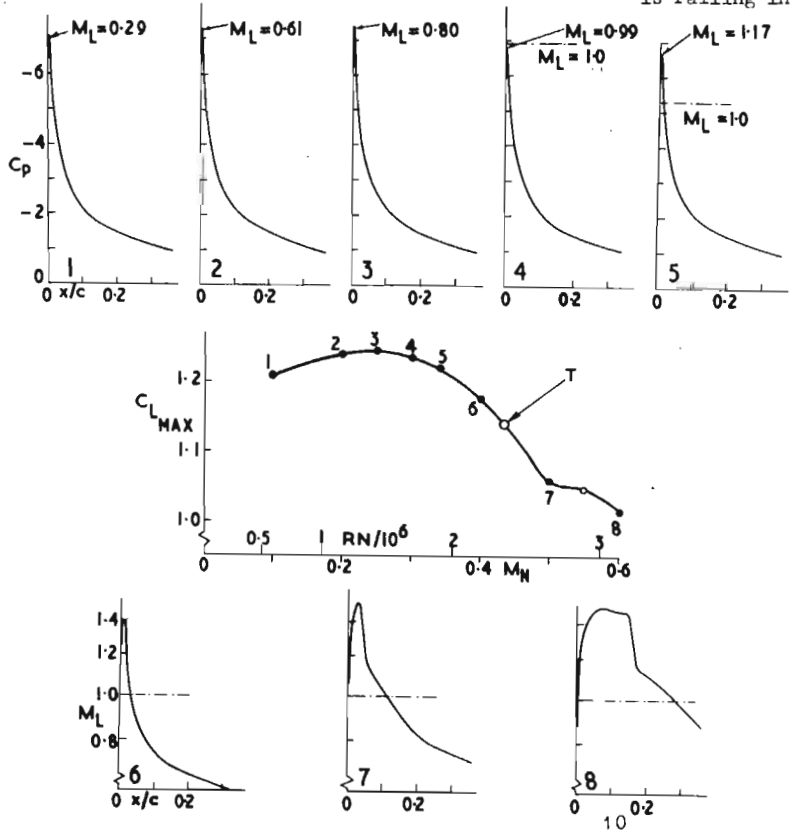

Figure 21. The transition from low-speed to shock-induced stall; $C_{L_{max}}$ and upper-surface leading-edge pressures.

but rising in terms of local Mach number to a value of 1.4 at point 6. By this stage, therefore, one might expect shock-induced separations of the type revealed by Fig's 6 and 20 to be playing some part in the flow processes. This is confirmed by the fact that the Mach number for which $C_{L_{max}}$ occurs at 12° (point T on Fig.21) is 0.435 - just the stage at which the shock-induced bubble begins to grow rapidly (see Fig.20). (It is clear, by contrast, that the early influence of Mach number, for maximum local Mach numbers just below and just above 1.0, must occur through some other mechanism). For higher stream Mach numbers, around M=0.5, (point 7), the local supersonic flow begins to extend noticeably rearwards; the associated extra lift is reflected in the shape of the $C_{L_{max}}$ variation.

At this point, it becomes especially appropriate to consider briefly the transformation from the aerofoil to a swept wing, but confining this still to the idealised yawed wing transformation - and remembering that the degree of idealisation is never insignificant. As explained above, this can be done on the basis of loci of constant M^2C_L.* Thus in Fig.22 the cruise

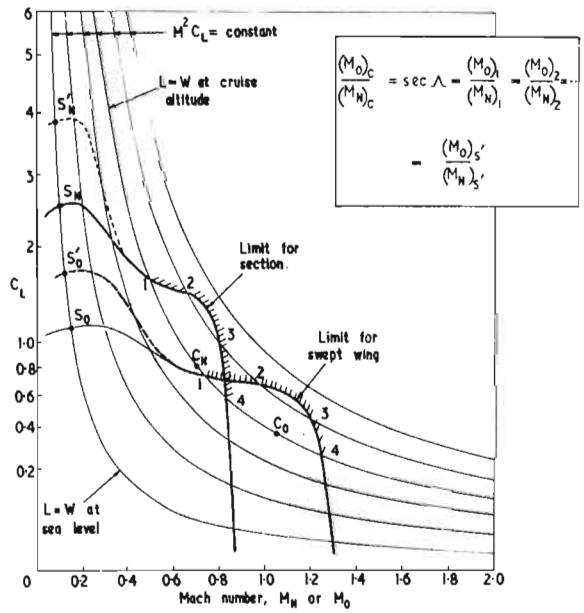

Figure 22. The idealised yawed-wing transformation from section to swept wing (see text).

condition, C_N, for the aerofoil moves along its line of constant M^2C_L to C_O, the cruise point for the swept wing, defined by the transformation ratio $M_O/M_N=\sec\Lambda$. All other corresponding points, such as those on the limiting boundaries are transposed by the same transformation ratio.* Since the lines of constant M^2C_L also indicate the maneouvre loads, etc., that are available, this transformation retains the nature of the flight envelope inferred from the section data.** This is known to be qualitatively reasonable and therefore a useful guide - at least for moderate degrees of sweepback - when the limiting boundary is defined by a straightforward shock-induced separation. However, it is obvious from Fig.22 that this cannot be so for the low-speed stall; the values of $C_{L_{max}}$ actually used on current swept wings correspond to points that would be well beyond the stalling conditions in two dimensions (boundaries that would correspond on the yawed-wing transformation are identified by lines that are either continuous or broken; the thin lines represent the respective unrealistic cases). There are various reasons for this, including the possibility of a vortex reattachment on the swept wing[1]. Here, then, is yet a further feature of special interest in the study of the influence of extremely small regions of local supersonic flow that dominate the stall in a range of speeds lying between those for the conventional low-speed stall and those for the conventional shock-induced one.

5. Transonic flows on helicopter blades

This is a convenient stage at which to transfer the discussion to helicopter blades, because some of the more recent contributions in this field have highlighted the part played by the same very small regions of embedded supersonic flow in stalling the retreating blade and through this in limiting the forward speed, manoeuvrability, etc.[4] (Fig.23). Attention has been drawn also to

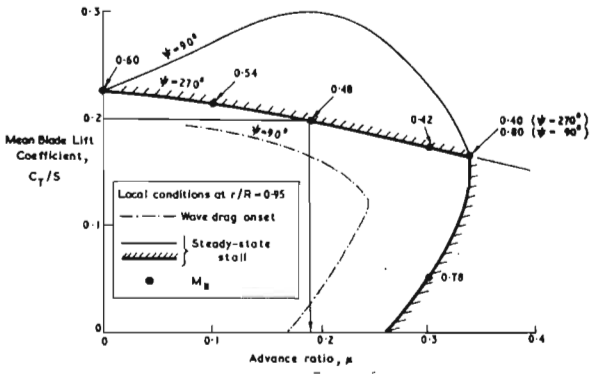

Figure 23. Helicopter forward speed limited (μ=0.19) by retreating blade stall (Ref. 4).

the manner in which the available maximum loading is augmented by the fact that the blade elements are yawed to the resultant flow direction[3]. These papers and others illustrate the nature of the gap between the idealisation represented by the two-dimensional aerofoil in steady flow and the actual conditions experienced on the blade elements of real rotors in their three-dimensional, periodic environment. They show how the gap can be bridged in rotor design by engineering solutions that allow for the effects of yaw and rate of change of incidence on $C_{L_{max}}$[3], and demonstrate that shock-induced separation is indeed observed in flight at

*$M_N=M_O\cos\Lambda$, $C_{L_N}=C_L\sec^2\Lambda$, i.e. $M_N^2C_{L_N}=M_O^2C_L$

$M_O/M_N=\sec\Lambda=(M_O)_1/(M_N)_1$, ……$(M_O)_{S'}/(M_N)_{S'}$

**Incidentally it also shows the manner in which a stall could occur on a variable sweep wing if the sweep were to be changed without the appropriate changes in speed.

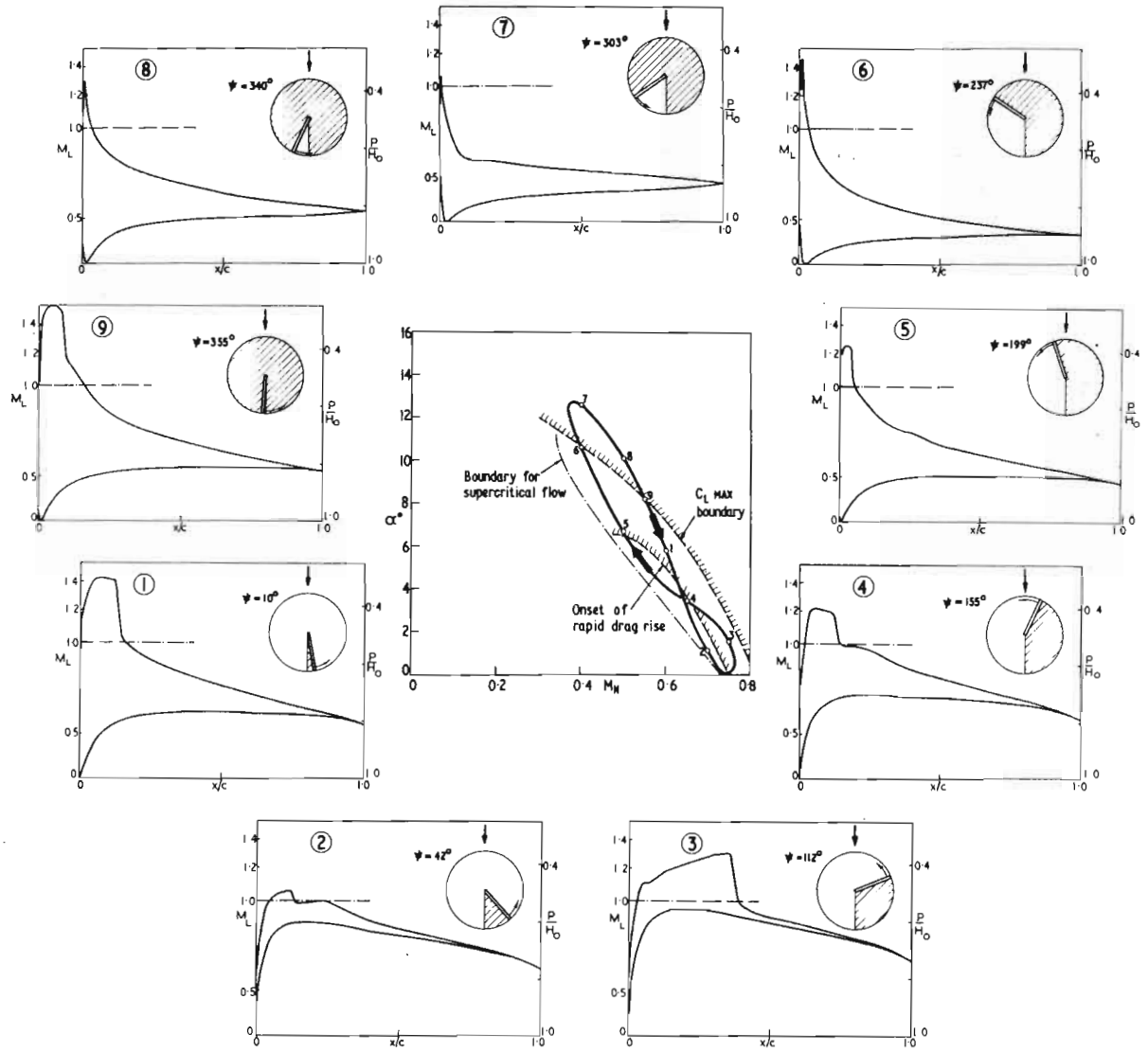

Figure 24. (Centre) Flow boundaries for NACA 0012 aerofoil and the locus of conditions for a blade element (0.93 radius) in forward flight. (Pheripheral) Steady-flow pressure distributions corresponding to numbered symbols on the locus.

the conditions that would be predicted by building aerofoil data into a comprehensive rotor computation(36).

With the real problems thus exposed, we can, as we did for the swept wing, feel safe in returning to the idealised two-dimensional aerofoil in steady flow for this brief, broad look at some of the basic ways in which transonic flows interact with blade design. J.P. Jones(4) used Fig.23 to demonstrate how the maximum forward speed available with a certain disc loading is restricted by retreating blade stall. Similar considerations would reveal how shock-induced separation reduces the limits on disc loading available in hover or in manoeuvre at any given forward speed. We will confine our attention here to the case of maximum forward speed.

Turning to Fig.24, the now familiar figure-of-eight loop drawn on the (α,M) plane of the central diagram is the locus of conditions that would be traced out in each revolution by the blade element at 0.93 radius with the rotor of an actual helicopter operating just beyond its design maximum forward speed.(19)+ In juxtaposition are the flow boundaries for the two-dimensional aerofoil, NACA 0012, used for the rotor blades of this particular helicopter. The peripheral diagrams give the chordwise surface pressure distributions measured in steady flow at the conditions corresponding to the nine numbered symbols on the locus.

It will be seen at once that the flow is supercritical over some regions of the upper surface for all (steady) conditions on the locus; in particular, the points 6, 7, 8, 9 for the

+ These conditions were derived by Westland Helicopters Ltd. using their rotor computation programme.

retreating blade are all on or beyond the boundary for $C_{L_{max}}$ in steady flow. The stall is entered at 6 (M=0.4) in just the sort of conditions for which, as discussed above, a separation of the type induced by very small shock waves (local M=1.4) is beginning to dominate the stall. At 9 on the other hand, where the locus is just recrossing the steady flow $C_{L_{max}}$ boundary, the steady conditions (M=0.55) are characterized by clearly established and classical shock induced separation.

At the beginning of the advancing sector (point 1), the (α,M) for the blade element in question, (5.8°, 0.6), would, in steady flow, generate a well-established supersonic region, with a fairly strong shock wave and significant wave drag locally. This collapses by point 2 (ψ=42°) and regrows again by point 3 (ψ=112°). A small patch of local supersonic flow remains for points 4 and 5, but is only just on the point of wave-drag rise. One would expect the repeated growth and collapse of supersonic flow, wave drag, shock induced separation and stalling to be modified for the dynamic case; nevertheless Tanner and Wohlfeld[36] have identified similar repeated changes on a rotor in flight at conditions predicted by a similar analysis based on aerofoil data. Their examples included even a case for which the critical local (α,M) conditions were induced at r/R=0.5 by the velocity field of the vortex of a preceding blade. As suggested by them, it would hardly be surprising if, an addition to performance and manoeuvre limitations, some of the noise and vibration problems encountered on rotors are produced by these repeated changes. Let us reiterate, nevertheless, that the illustrations that we have used were obtained for steady conditions of incidence and Mach number.

It is clear even from this one case that, in developing new aerofoil shapes for helicopter blades, one is necessarily concerned with the manner in which local supersonic flow accelerates and decelerates in a chordwise sense for a very wide range of conditions; the problems and features discussed in Section 3 assume considerable relevance. It is clear also that one is concerned with the type of shock-induced stall that is not very well understood (Section 4) as well as with the more classical types. Inclusion of the hover condition (usually beyond drag rise), and manoeuvre as well, means that one is confronted with an optimisation problem that is even more difficult than for a fixed wing aircraft. This is reflected in the differences in the shapes of the limiting boundaries for the aerofoils represented respectively in Fig's.24 and 7. For the wing case, emphasis can often be confined to the achievement of high loading in a part of the Mach number range, but, for the helicopter, more attention has to be paid to gains that are spread across the whole range. J.P. Jones[4] has illustrated one example in which this has been achieved on an aerofoil with cambered leading edge.

6. Transonic flows on nacelle lips

We referred in the Introduction to some of the many ways in which transonic flows are involved in the propulsion system and its installation. From this very wide field, some recent detailed observations of the flow on the lips of subsonic nacelles provide excellent examples around which to recapitulate briefly the main theme of our paper, namely, that transonic flows occur in a diversity of forms and circumstances and are responsible for many of the limitations to aircraft performance; these same examples are also appropriate to our two subsidiary themes, namely, that evolutionary progress can be made from studies of the basic flow phenomena (e.g. the wave cancellation in peaky flows), and that understanding is still poor for some of the phenomena that are of real pratical significance (e.g. very small regions of embedded supersonic flow and their repercussions).

The pressure distributions in Fig.25 have been redrawn - from results presented by Young[37] - to show directly the local Mach numbers (linear scale of pressure ratio, p/H) in the embedded regions of supersonic flow that develop on the lips of subsonic cowls, especially on the outer lip as mass-flow ratio, μ, into the intake is reduced at fixed values of the stream Mach number. This is the classical spillage case in which substantial proportions of the total thrust can be lost if the full suctions are not generated on the lip and if the deceleration from the high velocities is not accomplished without shock-wave drag and boundary-layer separation. It is associated with the variation of engine power and can occur for a very wide range of speeds, as is shown, for example, by the fact that high local Mach numbers are reached for the forward speed corresponding to M_o=0.7 as well as near cruise, M_o=0.82.

The degree of convex turning from the stagnation point (between the inner and outer flow) becomes very large for low values of the mass-flow ratio, and the local Mach numbers are therefore very high unless the kind of wave cancellation described in Section 3 is invoked in large measure. A significant degree of isentropic compression upstream of the shock is indeed apparent in the examples shown in Fig.25. Moreover, as mentioned in the Introduction, it was in this very context

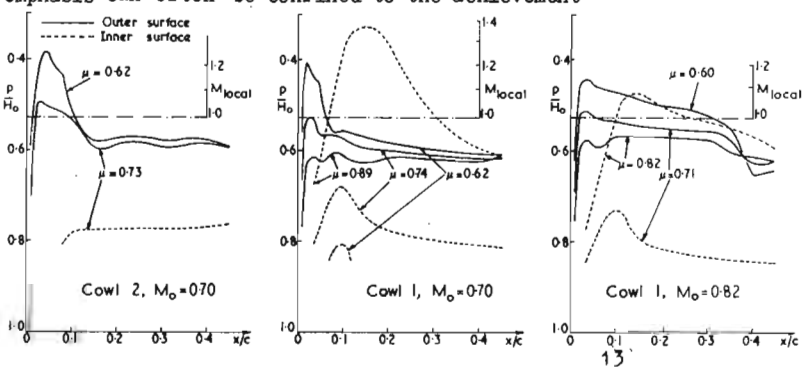

Figure 25. Surface pressures on nacelle lips for varying mass-flow ratio, μ, (Ref. 37); full lines - outer surface, broken lines - inner surface.

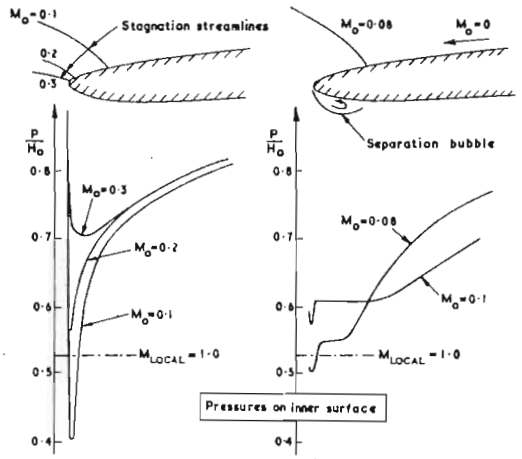

Figure 26. Pressures on the inner lip of a nacelle for high thrust and low speeds (Ref. 8).

that some of the earliest incidental observations of peaky flows were recorded, and, as illustrated by the results reproduced in Fig.4 from the Hawker Siddeley[9] account of the Harrier intake design, it is in this field that some of the most striking successes have been achieved in designing for peaky flows.

Of course, for the conventional nacelle the wave cancellation process and other features of the local supersonic flow will differ from those on the aerofoil[37] in that they will usually be tuned to axi-symmetric characteristics and to annular stream tubes instead of to two-dimensional ones. In relation to the values of local Mach number there is a tendency for shock waves to occur later on nacelles than on aerofoils, to be weaker and to grow in height less rapidly, but there can be no doubt about the qualitative similarity in the flow phenomena or about the fact that evolutionary progress stems from understanding them.

Small regions of embedded supersonic flow frequently occur on the inner lip of nacelles for an even greater range of forward speeds. This is shown for example in Fig.25 for cowl 1 at M_o=0.7, but even more dramatically in Fig.26[8]. Here, with the high engine power appropriate to acceleration for take off, the stagnation point between the outer and inner flow is well on the upper side of the lip, and the acceleration to the inner side is consequently high. A clear supersonic region is present at M_o=0.1, disappearing as the stagnation point comes round to the leading-edge with increasing forward speed. It is interesting also to trace the collapse of the suction peak as forward speed is reduced from M_o=0.1 to zero, with engine power remaining high; the similarity to the collapse that occurs for aerofoil stall is quite striking. Gregory[38] also observed local regions of supersonic flow on an intake running statically, some of them with small shocks and some without, some with separations and some without. Again, therefore, there can be no doubt that these very small supersonic regions - and the transition from the associated shock-induced boundary layer separations to those that are of the classical low-speed type - are qualitatively very similar to those that occur on aerofoils and wings. Their emergence in this context adds to the widespread significance of these very small regions and their repercussions, and provides yet another example to emphasise how further phenomenological studies could lead to evolutionary progress.

References

1. Küchemann, D., "Fluid Mechanics and aircraft design". 6th Nilakantan Memorial Lecture. Presented at Annual General Meeting of Aeronautical Society of India, March 1970.
2. Lock, C.N.H., Pankhurst, R.C., and Cann, J.F.C., "Strip theory method of calculation for airscrews on high-speed aeroplanes". A.R.C. R and M 2035 (1945).
3. Harris, F.D., Tarzanin, F.J., and Fisher R.K., "Rotor high speed performance, theory versus test". V/STOL Technology and planning conference, Las Vegas (1969).
4. Jones, J.P., "The helicopter rotor". 13th Lanchester Memorial Lecture of the Roy. Aero. Soc. (April 1970). To be published in J. Roy. Aero. Soc.
5. Miller, G.R., and Hartmann, M.J., "Experimental shock configurations and shock losses in a transonic compressor at design speed". NACA RM E58A 14b (1958).
6. Hetherington, R., "The aerodynamics of engine component design problems associated with large subsonic aircraft". AGARD-LS-37-70 (1970).
7. Carrière, P., "Effets de l'écoulement interne sur le comportement aerodynamique d'un avion a réaction". 6th Congress of I.C.A.S., Munich (1968).
8. Leynaert, J., and Meauze, G., "Some problems of transonic flow for engine nacelles of airbus type aircraft". AGARD Conference Proceedings No. 35 (1968).
9. Fozzard, J.W., Bore, C et al., "Hawker Siddeley Harrier". Aircraft Engineering, Vol. XLI, No. 12, Dec. 1969 and "Air intakes of the Hawker Siddeley Harrier" - Hawker Siddeley Technical Review, Vol. 5, No. 3 (1970).
10. Küchemann, D., and Weber, J., "Aerodynamics of Propulsion". McGraw Hill (1953).
11. Bagley, J.A., "Wind tunnel experiments on the interference between a jet and a wing at subsonic speeds". AGARD Conference Proceedings No. 35 (1968).
12. Kutney, J.T., and Piszkin, S.P., "Reduction of drag rise on the Convair 990 airplane" - Journ. Aircraft. Vol. 1, No. 1, (1964).
13. Haines, A.B., "Recent research into some aerodynamic design problems of subsonic transport aircraft". 6th Congress of I.C.A.S, Munich (1968).
14. Nieuwland, G.Y., "Theoretical design of shock-free, transonic flow around aerofoil sections". 5th Congress of I.C.A.S., London (1966). Aerospace Proceedings, Macmillan (1967).
15. Yoshihara, H., Carrière, P et al., "Transonic Aerodynamics". AGARD Conference Proceedings No. 35 (1968).

16. Germain, L.P., "Actualité des problèmes transsoniques". Proc. Canadian Congress of Applied Mechanics (1967) (also O.N.E.R.A. T.P. 513).

17. Murman, E.M., and Cole, J.D., "Calculation of plane steady transonic flows". Boeing S.R.L. Document D1-82-0943 (1970).

18. Nieuwland, G.Y., and Spee, B.M., "Transonic shock-free flow, fact or fiction?" AGARD Conference Proceedings No. 35 (1968).

19. NPL Annual Report 1968-9.

20. Pearcey, H.H., Contribution to discussion of Ref. 14.

21. Pearcey, H.H., "The aerodynamic design of section shapes for swept wings" - 2nd Congress of I.C.A.S., Zurich (1960), Advances in Aeronautical Sciences, Vol. 3, Pergamon Press.

22. Pearcey, H.H., "Shock-induced separation and its prevention by design and boundary-layer control". Part IV Boundary Layer and Flow Control (Ed Lachmann), Pergamon Press (1960).

23. Hay, J.A., "Vickers V.C.10. Part 1 - Aerodynamic Design". Aircraft Engineering, Vol. XXXIV, 1962 p.158.

24. "Hawker Siddeley Trident, Aerodynamic design and flying controls" - Aircraft Engineering, Vol. XXXVI, 1964, p.172.

25. NPL Annual Report 1966.

26. Roy. Aero. Soc. T.D.M. 67009.

27. NPL Annual Report 1963.

28. Spee, B.M., and Uijlenhoet, R., "Experimental verification of shock free transonic flow around quasi-elliptical aerofoil sections". 6th Congress of I.C.A.S., Munich (1968).

29. Shapiro, A.H., "The Dynamics and Thermodynamics of Compressible Fluid Flow". Ronald Press (1954).

30. Thompson, N., Wilby, P.G., "Leading-edge supersonic velocity peaks and the determination of the velocity distribution on an aerofoil in a sonic stream" - AGARD Conference Proceedings No. 35 (1968).

31. Graham, W.J., "A method for the calculation of the flow about blunt leading-edge aerofoils at sonic speed". NPL Aero Report 1179 (1966).

32. Wilby, P.G., "The pressure drag of an aerofoil with six different round leading-edges, at transonic and supersonic speeds" - ARC Current Paper 921 (1966).

33. Erlich, E., "Examples de recherches sur les profils dans la soufflerie S10 du C.E.A.T. a Toulouse" - A.F.I.T.A.E., VI^{e} Colloque d'Aérodynamique Appliquée, Toulouse, 1969. (O.N.E.R.A. T.P. 766).

34. Vincent de Paul, M., "Experimental research on supercritical wing profiles" - AGARD Conference Proceedings No. 35 (1968).

35. Wootton, L.R., "The effect of compressibility on the maximum lift coefficient on aerofoils at subsonic airspeeds" - J. Roy. Aero. Soc., Vol. 71, 1967.

36. Tanner, W.H., and Wohlfield, R.M., "New experimental techniques in rotorcraft aerodynamics and their application". J. American Helicopter Society, Vol. 15, No. 2, April 1970.

37. Young, C., "An investigation of annular aerofoils for turbofan engine cowls" - R.A.E. Tech. Rep. 69285 (1969).

38. Gregory, N., "On the static performance of two-dimensional intakes with momentum injection in the form of boundary-layer control by blowing" - NPL Aero Special Report 006 (1968) (to be published as ARC R and M).

39. Pearcey, H.H., Osborne, J., and Haines, A.B., "The interaction between local effects at the shock and rear separation - a source of significant scale effects on aerofoils and wings". AGARD Conference Paper No. 35 (1968).